

GEOMETRICAL SHIFT RESULTS IN ERRONEOUS APPEARANCE OF LOW FREQUENCY TISSUE EDDY CURRENT INDUCED PHASE MAPS: THEORY, SIMULATIONS AND MEASUREMENTS

S. Mandija¹, A.L.H.M.W. van Lier¹, P. Petrov², S.W.F. Neggers², P.R. Luijten¹, and C.A.T. van den Berg¹

¹Imaging Division, UMC Utrecht, Utrecht, Netherlands, ²Brain Center Rudolf Magnus, UMC Utrecht, Utrecht, Netherlands

Introduction: Being able to electrically characterize tissues in the 0.1-10 kHz range is relevant for various biomedical purposes, e.g. to calculate the current induced in transcranial magnetic stimulation therapy. For this purpose, in MR Electrical Impedance Tomography (MR-EIT) a current is injected in tissues using skin electrodes and from the accumulated MR signal phase related to electric currents, electric conductivity maps can be created⁽¹⁾. To reduce pain sensation due to the high current injected in MR-EIT, other studies have suggested to use MR time-varying gradient fields where eddy currents are inductively induced by time-varying gradients⁽²⁾. However, electromagnetic simulations indicate that the accumulated low frequency (LF) phase due to induced currents by time varying gradient fields should be very small (μ rad), thus hardly measurable⁽³⁾. Here we demonstrate that through a geometrical error along the readout direction, RF phase leaks in the LF phase when phase images of different gradient polarity are summed or subtracted, completely overshadowing the LF phase. Since the RF phase is related to conductivity at MHz frequency, because of this geometrical displacement it appears that the LF phase is also proportional to electrical conductivity.

Theory: Phase images: The measured accumulated phases for opposite readout gradient polarities are defined as: $\Phi_{acc}^+ = +\Phi_{RF} + \Phi_{eddy_phantom} + \Phi_{eddy_system}$, $\Phi_{acc}^- = +\Phi_{RF} - \Phi_{eddy_phantom} - \Phi_{eddy_system}$, where Φ_{RF} is the radiofrequency phase contribution, Φ_{eddy_system} is the phase contribution due to system eddy currents and $\Phi_{eddy_phantom}$ is the phase contribution due to tissue eddy currents, which is zero if the phantom has zero conductivity (reference phantom). From these equations, the RF phase map and the accumulated phase map due to LF phantom eddy currents induced by the ramp up of the readout gradient are reconstructed: $\Phi_{RF} = (\Phi_{acc}^+ + \Phi_{acc}^-)/2$, $\Phi_{LF_phantom} = ((\Phi_{acc}^+ - \Phi_{acc}^-)_{\sigma \neq 0} - (\Phi_{acc}^+ - \Phi_{acc}^-)_{\sigma=0})/2$ ⁽⁴⁾.

Pixel shift model: In Fig. 1 (right part), a pixel shift in the readout direction is observed. From the Fourier's shift theorem, a phase offset ($\Phi_0 = k_x x_0$) caused by B0 distortions leads to a shift in the image along the readout: $\hat{p}(x - x_0, y) = \int_0^{TE} s(k_x, k_y) e^{i2\pi(k_x(x-x_0) + k_y y)}$. This shift causes Φ_{RF} leakage in $\Phi_{LF_phantom}$ (Φ_{RF}^{leak}) while calculating $\Phi_{acc}^+ - \Phi_{acc}^-$, as complex data of different locations are combined. As we will demonstrate below, this can completely explain the observed LF phase.

RF Conductivity reconstruction: We reconstruct the RF conductivity σ_{RF} , noticing that this artefact has no impact on it (Fig. 2 a, b, c and d), and showing why also the LF phase, that is scaled with Φ_{RF}^{leak} , appears conductivity related. Since Φ_{RF} has a parabolic shape, to retrieve σ_{RF} from the corrected Φ_{RF} (Fig. 2 c-d) we

use a parabolic model for each direction ($d = x, y$, and z respectively): $\Phi_{RF} = ad^2 + bd + c$ (Fig. 2 e-f), where "a" is the parameter conductivity related. Since $\sigma_{RF} \approx (\nabla^2 \Phi_{RF})/\mu\omega$, with $\psi_+ = \Phi_{RF}/2$ in quadrature Tx/Rx mode⁽⁵⁾, we obtain $\sigma_{RF} \approx a/\mu\omega$ ⁽⁶⁾.

Materials and methods:

Phantoms: two cylindrical conductive phantoms (Fig. 2 g-h), and one non-conductive (to compensate for system eddy currents): $r = 4.3\text{mm}$, $L = 200\text{mm}$.

Simulations: $\Phi_{LF_phantom}$ is simulated (Fig. 2, i-j) assuming for phantoms the same position and orientation used for measurements. First, we define an incident vector potential \mathbf{A}^{inc} to simulate the incident magnetic field due to the ramp up of a readout gradient along x ⁽⁷⁾. Then, by applying a quasi-static approximation, we calculate the current density \mathbf{J}^{ind} induced by \mathbf{A}^{inc} . Finally, using Biot-Savart's law, we calculate the magnetic field \mathbf{B}^{ind} induced by \mathbf{J}^{ind} , and then we calculate $\Phi_{LF_phantom}$, where $\Phi_{LF_phantom} = 2\pi\mathbf{B}^{ind} \cdot \mathbf{TE}$.

Measurements: We performed Multi Spin Echo experiments in a 3T MR scanner (Achieva, Philips Healthcare, Best, Netherlands). In Fig. 1 (right part), we observe a non- perfect overlapping due to one pixel shifts in the opposing readout directions between Φ_{acc}^+ and Φ_{acc}^- (Fig.1 left and center parts). This shift is independent from the gradient strength, thus is probably related to zero order eddy currents flowing in the system. This effect is clearly visible in Φ_{RF} (Fig. 2 a-b) and $\Phi_{LF_phantom}$ (Fig. 2 k-l) (red-blue external rings). To obtain correct maps of Φ_{RF} and $\Phi_{LF_phantom}$ (Fig. 2, c, d, m and n) a shift of one pixel along the readout direction is necessary in post-processing for either Φ_{acc}^+ or Φ_{acc}^- . Then we evaluate the contribution of Φ_{RF}^{leak} if correction in post-processing is not performed. This contribution is obtained by subtracting the corrected and non-corrected Φ_{RF} maps (Fig. 2 o-p). Finally, we compare Φ_{RF}^{leak} with the pre-correction $\Phi_{LF_phantom}$ measurements, for different conductive phantoms (Fig. 2 q-r), and for the same phantom using a different readout slew rate (Table and Fig. 3).

Results: Φ_{RF} corrected for the one pixel shift maintains its parabolic shape, it is scaled with the conductivity (Fig. 2 e-f), and the reconstructed conductivity well reflects the expected values (Fig. 2 g-h). From simulations (Fig. 2 i-j), we predict that $\Phi_{LF_phantom}$ is not measurable since it is four orders of magnitude lower than the measured one (Fig. 2 k-l). In fact, after correcting for one pixel shift (Fig. 2 m-n), $\Phi_{LF_phantom}$ maps do not show the simulated pattern. If we compare Φ_{RF}^{leak} (Fig. 2 o-p) with the non-corrected $\Phi_{LF_phantom}$ (Fig. 2 k-l) we see that they both match perfectly for different values of conductivities (Fig. 2 q-r) and they are linearly scaled with it. From Faraday's induction law it follows that, different slew rates would induce different current densities and therefore different $\Phi_{LF_phantom}$ maps. Instead, in the two experiments in Fig. 3, the non-corrected $\Phi_{LF_phantom}$ maps (Fig. 3 a-d) do not scale with different slew rates (obtained modifying $G_{readout}$) but they perfectly match with Φ_{RF}^{leak} (Fig. 3 b-e). Therefore employing stronger gradients to measure $\Phi_{LF_phantom}$ is not useful. In fact, as we show in simulations, this phase is too small respect to Φ_{RF}^{leak} . Thus we can demonstrate that the non-corrected $\Phi_{LF_phantom}$ pattern, that is scaled with σ_{RF} , can be completely attributed to Φ_{RF} .

Discussions and Conclusions: After correcting for the pixel shift, the noise level hides $\Phi_{LF_phantom}$ (Fig. 2 m-n) since this phase, as predicted in simulations, is too small to be measured. Instead, if this correction is not performed, the leakage of the Φ_{RF} in the $\Phi_{LF_phantom}$ is measured. As demonstrated, this effect can completely explain the measured $\Phi_{LF_phantom}$ maps. The scaling of the non-corrected $\Phi_{LF_phantom}$ with the conductivity, that up to now was supposed to be related to the different levels of induced eddy currents, can be attributed instead to the RF phase leakage, whose contribution is dependent on the RF conductivity. RF conductivity estimates through EPT reconstruction, is hardly affected by geometrical displacement artifact. In conclusion, combinations of phase maps obtained with different gradient polarities should be done carefully since these images are prone to geometrical shift leading to RF phase falsely attributed to LF phase. Our result indicate that even a sub-pixel geometrical shift can cause significant Φ_{RF}^{leak} , eclipsing completely $\Phi_{LF_phantom}$.

References: [1] E. Woo et al, Physiol. Meas. 2008, 29, 1-26. [2] van Lier et al, ISMRM 20, 2012, 3467. [3] E. Gibbs et al, POSTER 3rd International Workshop on MRI Phase Contrast & Quantitative Susceptibility Mapping. [4] M. A. Bernstein et al, Handbook of MRI Pulse Sequence, Elsevier, 2004. [5] van Lier et al, Magn Reson Med 2012, 67, 552-561. [6] U. Katscher et al, IEEE Trans. Med. Imaging 2009, 28 (9), 1365-1374. [7] S. Mandija et al, ISMRM 2014, 0639.

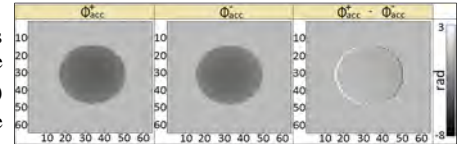


Figure 1: phase maps for opposite readout gradient polarity (left and center). Opposite pixel shift artefacts for different gradient polarities visible after subtracting the two phase maps: white/dark gray pixels (right).

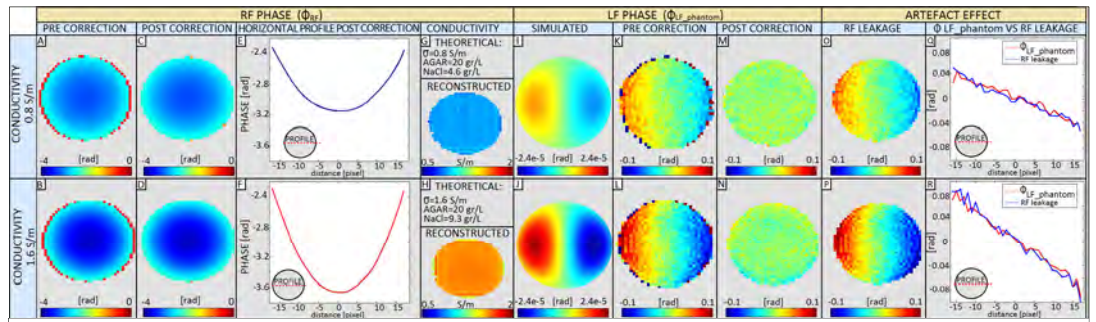


Figure 2: RF and LF phase maps pre and post correction, and effect of the pixel shift for two different conductive phantoms.

EXP.	TR (ms)	TE (ms)	WFS/BW (pix/Hz)	Tramp (ms)	Greadout (mT)	Slew Rate (T/m/s)	Pixel (mm)
1	1	4.5	0.140/3006	0.155	29.185	188.29	2.5x2.5x2.5
2	1	4.5	0.465/934	0.155	8.78	56.65	2.5x2.5x2.5

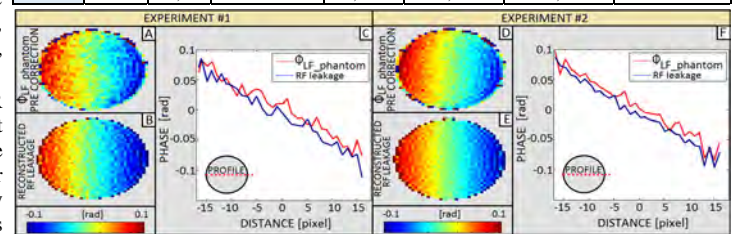


Figure 3: Comparison between Φ_{RF}^{leak} and non-corrected $\Phi_{LF_phantom}$ for different slew rates.